


Applying Common Equations of State to Three Reference Fluids: Water, Carbon Dioxide, and Helium

Martin König and Markus Weber Sutter*

DOI: 10.1002/cite.202100004

 This is an open access article under the terms of the Creative Commons Attribution-NonCommercial-NoDerivs License, which permits use and distribution in any medium, provided the original work is properly cited, the use is non-commercial and no modifications or adaptations are made.



Supporting Information
available online

Thermodynamic properties such as density, vapor pressure, heat of evaporation, and the speed of sound for three pure reference fluids were computed applying various common equations of state over a fairly wide range of pressures and temperatures. The results obtained by rather basic equations of state were held against those from sophisticated reference equations, and contour plots were drawn indicating the respective error margins. Thereby, it was quantitatively illustrated within which limits cubic equations of state can be used for reasonably accurate calculations of various properties.

Keywords: Equations of state, Safety valves, Speed of sound

Received: January 13, 2021; *revised:* June 23, 2021; *accepted:* June 24, 2021

1 Introduction and Purpose of this Paper

Determining various volumetric properties of a fluid phase by computational algorithms has become a subordinate part in many cases of contemporary modeling work on thermodynamic systems and processes. Since the pioneering work of van der Waals [1, 2], it is widely accepted that for each pure substance a wide range of pressures and temperatures even encompassing the two-phase region by a large margin can be covered by making use either of one single volumetric equation of state combined with a caloric equation of state or of one fundamental equation of state. As any novice in this field will find out soon, for most fluids there is not just one such equation available but rather a whole variety from which to choose the most suitable one. To determine which of the numerous equations of state will most likely meet the accuracy requirements while absorbing only a minimum of CPU power is a rather preliminary, though often underestimated problem. The purpose of this review is to present a comparative survey of the most commonly used equations of state, thereby educating the interested reader about the process in which these equations were subsequently developed and about the accuracy and reliability of the results obtained from their application.

1.1 Early and Fundamental Development of Equations of State

On the basis of experimental studies and well-founded theoretical investigations, a large variety of equations of state (henceforth abbreviated as EoS or EoSs) have been developed. Fig. 1 shows a choice of EoSs and some of the well-known theories that decisively influenced their performance. While the diagram in Fig. 1 is far from being exhaustive, especially when it comes to more recent developments where numerous researchers have made very valuable contributions, we maintain that protagonists of a theory or technique are named and their impact is duly acknowledged.

When the findings of Avogadro, Gay-Lussac, and Boyle and Mariotte were combined first, this resulted in the formulation of the ideal gas law [3].

$$PV = RT \Leftrightarrow P = \frac{RT}{V} \quad (1)$$

Eq. (1), which became the basis of all further investigations and theories, correlates the pressure P exerted on the

Martin König and Prof. Dr. Markus Weber Sutter
markus.weber@zhaw.ch
Zurich University of Applied Sciences, ZHAW, Institute of Energy Systems and Fluid Engineering, Technikumstraße 9, 8400 Winterthur, Switzerland.

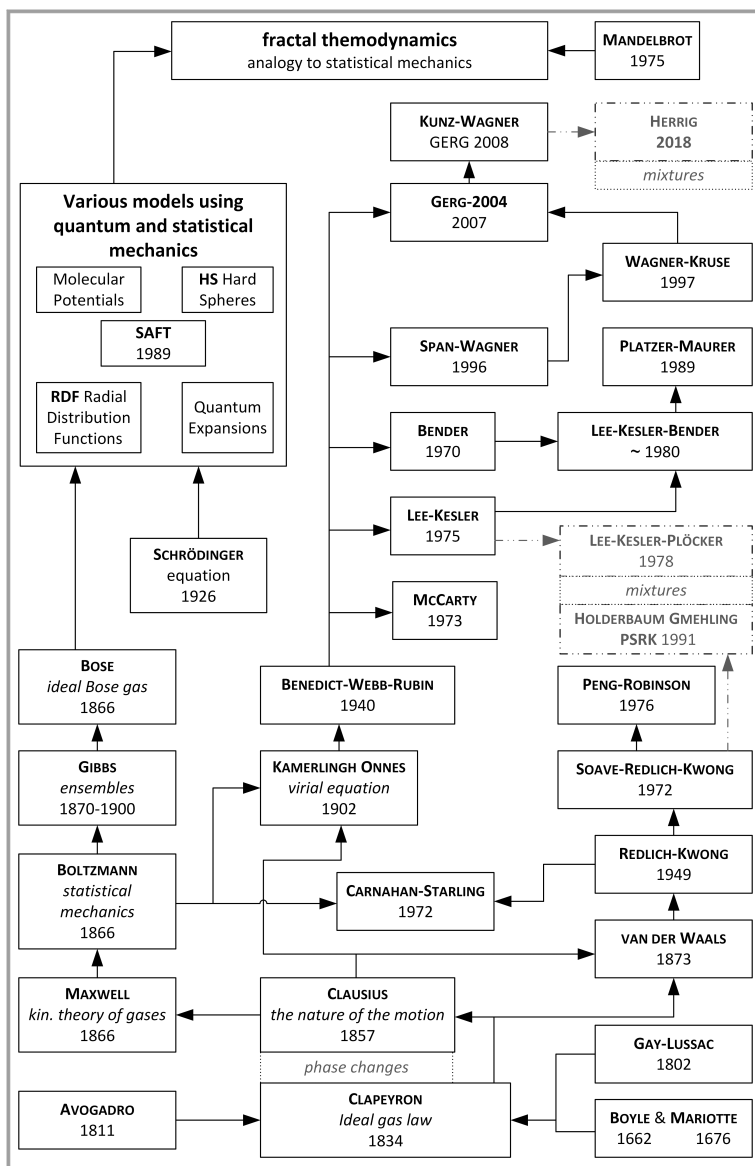


Figure 1. Representation of selected equations of state, their mutual relations, their underlying approaches, and their evolution over time.

inner walls of a container with the molar volume V and the temperature T at which the gas is held inside of this container through the universal gas constant R .

Observation and theoretical description of molecular motions laid ground to a new way for Clausius to describe the essence of heat [4]. Advanced studies of particle movement opened out into a branch on its own of both development of EoSs and theories on the thermodynamic behavior of fluid matter. Following these ideas, Maxwell developed first the kinetic theory of gases [5] before Boltzmann made his contributions to what Gibbs later called statistical mechanics, which he amply employed to fundamentally describe thermodynamic systems [6–8]. Later on, models making use of quantum physics [9, 10] or fractals [11, 12] were devel-

oped. However, these types of fundamental considerations are rather complicated and extensive, why we decided to add more weight to classical continuum descriptions, in which the temperature T , the specific volume V , and the pressure P are the primary independent variables.

1.2 Specific and Workable EoSs

In 1873, van der Waals [1] was the first scientist to introduce an EoS with the built-in capacity to successfully describe a continuous transition between the gaseous and the liquid state of a pure fluid as well as to predict the existence of a two-phase region separating these two states at subcritical temperatures. His achievements are all the more remarkable as the two additional constants that he used to establish his EoS are directly derived from basic findings about molecules and how they build up pressure when being enclosed in a chamber of defined size at a given temperature, i.e., in a given state of thermodynamic excitation. Pressure can be considered as being built up by two separate contributions that are superimposed, namely, one by repulsive forces and one by attractive forces.

$$P = P_{rep} + P_{attr} \tag{2}$$

Supposing that the repulsive forces were related to a certain “inaccessible” volume b of the molecules while the attractive forces were due to molecule-to-molecule interactions and, therefore, inversely proportional to the specific volume squared, van der Waals [1, 2] proposed Eq. (3), which later would be accounted as the first cubic equation of state. When solving Eq. (3) for V at any given set of P and T , a polynomial equation of third order in V emerges, always having three roots out of which at least one would be real.

$$P = \frac{RT}{(V - b)} - \frac{a}{V^2} \tag{3}$$

Eq. (3) is entered by not more than two fluid-specific constants that are to be derived from critical data. And while it is successful in predicting the existence of a two-phase region as well as the upper end of the vapor pressure function, i.e., the pressure P_c and the temperature T_c at the critical point, it generally fails at correctly predicting a realistic slope of the vapor pressure function, the liquid densities at the border of the two-phase region, and the specific volume V_c at the critical point. According to Eq. (3), all fluids should have an identical critical compressibility factor of $Z_c = 3/8$. While this value is off by some 25 % for most

fluids, the idea that Z_c was virtually identical for all fluids, and thus a rather universal property, proved realistic for a vast majority of chemical species and, therefore, laid ground to the theory of corresponding states. Improvements to van der Waals' EoS were made by several authors over roughly one century. Introducing the acentric factor according to Pitzer, ω , [13] allowed for temperature dependence of the attractive term and, thereby, helped to adjust the slope of the vapor pressure function.

While, with the arrival of the Redlich-Kwong EoS and others, the critical compressibility factor Z_c shifted towards values that were more realistic, the issue with the fluid densities of the liquid phase at equilibrium conditions still persisted to some extent.

As always, what was or is considered a shortcoming of an EoS is closely related to the kind of prediction or modeling work intended. If all that needs to be known for the design of a technical process or application is the equilibrium vapor pressure of a pure fluid at a given temperature, then – the ideal gas law being out of question – van der Waals' EoS does at least predict a vapor pressure for any subcritical temperature although one that is far from being accurate in most cases, while any cubic EoS operating with a third substance-specific parameter (most commonly Pitzer's factor ω) will provide sufficiently accurate results for nonpolar substances. If, however, the technical application envisioned combines thermodynamic phenomena with aspects of fluid mechanics, the volume fractions of either phase at equilibrium and, hence, their densities must be known. Here, classical cubic EoSs typically fail by systematically under-predicting the density of the liquid phase while giving reasonably accurate densities (within a few percent or less) for the gas phase. As the technical application considered evolves into rather complex processes of energy conversion such as a refrigeration cycle or into a compressible-flow problem, caloric properties and their derivatives such as the speed of sound or the Joule Thomson coefficient of the fluid play a key role. In a classical setup where a volumetric EoS is combined with the ideal-gas isobaric heat capacity, the need for accurate numerical values for said derivatives implies the necessity of an even more accurate representation of the volumetric properties of a pure substance as well as of its caloric properties (which, in this classical constellation, is a subject of its own and structurally independent of the former). Numerous attempts have been made in the past to cure or improve cubic equations under this aspect. None of them was able to match the improvements made later when completely different approaches were developed.

The improvements achieved by replacing the well-established repulsive term by a hard-sphere function as derived by Carnahan and Starling [14] were primarily compelling when applied to mixtures [15]. Let alone that solving the respective EoS for V had now turned from finding the roots of a cubic equation into finding those of an equation of fifth order. This somehow symbolizes the dead end of the road for cubic EoSs, which nowadays are still strongly favorable

when being applied to mixtures for the calculation of vapor-liquid equilibria at elevated pressures [16].

It was van der Waals' successor at Leiden University, Kamerlingh Onnes, who, inspired by the work of Clausius [4] and Boltzmann, presented what is referred to as the first virial EoS in 1901 [17]:

$$Z = \frac{PV}{RT} = 1 + \frac{B(T)}{V} + \frac{C(T)}{V^2} + \frac{D(T)}{V^3} + \dots \quad (4)$$

$$P = \frac{RT}{V} \left[1 + \frac{B(T)}{V} + \frac{C(T)}{V^2} + \frac{D(T)}{V^3} + \dots \right] \quad (5)$$

The mechanistic idea (which is now abandoned) that all molecular interactions combined could be described as the superposition of interactions between couples, triplets, quadruplets, etc. of molecules was thereby seemingly expressed. The virial EoS laid the foundation of the third branch of developments. Benedict, Webb, and Rubin [18] took on the virial approach introduced by Kamerlingh Onnes and proffered an EoS using eight independent constants, $A_0, B_0, C_0, a, b, c, \alpha$, and γ , containing an exponential term for the first time:

$$P = \rho RT + \rho^2 \left(RTB_0 - A_0 - \frac{C_0}{T^2} \right) + (bRT - a)\rho^3 + \alpha a \rho^6 + \frac{c \rho^3}{T^2} (1 + \gamma \rho^2) e^{-\gamma \rho^2} \quad (6)$$

where ρ is the inverse of the specific molar volume V . This opened the door to more and more elaborate EoSs, the so-called multi-parameter equations of state (MPEoSs) [19].

Eq. (7) is the EoS according to Bender.

$$P = \rho T \left[R + B\rho + C\rho^2 + D\rho^3 + E\rho^4 + F\rho^5 + (G + H\rho^2)\rho^2 e^{-a_2 \rho^2} \right] \quad (7)$$

$$\text{wherein } B = a_1 - \frac{a_2}{T} - \frac{a_3}{T^2} - \frac{a_4}{T^3} - \frac{a_5}{T^4}, \quad C = a_6 - \frac{a_7}{T} - \frac{a_8}{T^2}, \\ D = a_9 - \frac{a_{10}}{T}, \quad E = a_{11} - \frac{a_{12}}{T}, \quad F = \frac{a_{13}}{T}, \quad G = \frac{a_{14}}{T^2} + \frac{a_{15}}{T^4} + \frac{a_{16}}{T^5}, \\ \text{and } H = \frac{a_{17}}{T^2} + \frac{a_{18}}{T^4} + \frac{a_{19}}{T^5}.$$

The Bender EoS was later generalized by Platzer and Maurer [20] who replaced the fluid-specific constants a_1 to a_{20} by polynomials in ω and χ as given in Eq. (8).

$$a_i = g_{4,i} + g_{1,i}\omega + g_{2,i}\chi + g_{3,i}\omega\chi + g_{5,i}\chi^2 \quad (8)$$

With this generalization, the number of independent fluid-specific constants besides P_c and V_c was brought down from twenty to two, where the Stiel factor χ was the only one that had to be dealt with in addition to the already established acentric factor ω . Both of these parameters are derived from the vapor pressure function (see Eqs. (13) and

(15)). The numerical values for the 95 constants $g_{j,i}$ in Eq. (8) are available from a universal table.

Another MPEoS is the one of Lee and Kesler [21], in which the compressibility factor Z is a weighted average of a rather ideal part $Z^{(0)}$ related to argon (referred to as simple fluid) and a residual part $Z^{(r)}$ taken from n -octane (referred to as reference fluid). Here, ω is the only fluid-specific constant and $Z^{(0)}$ as well as $Z^{(r)}$ are functions of the dimensionless specific molar volume, $V_r = VP_c/RT_c$ and the reduced temperature $T_r = T/T_c$, respectively.

$$Z = Z^{(0)} + \frac{\omega}{\omega^{(r)}} \left(Z^{(r)} - Z^{(0)} \right) \quad (9)$$

$$Z = \left(\frac{P_r V_r}{T_r} \right) = 1 + \frac{B}{V_r} + \frac{C}{V_r^2} + \frac{D}{V_r^3} + \frac{c_4}{T_r^3 V_r^2} \left(\beta + \frac{\gamma}{V_r^2} \right) e^{\frac{-\gamma}{V_r^2}} \quad (10)$$

Solving Eqs. (9) and (10) for Z requires one separate set of the constants B, C, D, c_4, β , and γ for $Z^{(r)}$ and $Z^{(0)}$ as well as an additional reference value of $\omega^{(r)} = 0.398$, which is Pitzer's factor attributed to n -octane.

The technical viability of MPEoSs, i.e., their computability, also set the stage for a novel approach in which it was no longer necessary to combine a volumetric EoS (much like the ones introduced so far) with a caloric EoS (typically of the format $C_p^0 = C_p^0(T)$). Rather, the two constituents were to be analytically combined to give so-called fundamental EoSs, mostly of the type $F = F(V, T)$ or $G = G(P, T)$, where the specific Helmholtz or Gibbs energies are complex polynomials of two independent variables, while any other variable of state is obtained from derivatives of these functions or combinations thereof. This way, Wagner and Kruse came up with the IAPWS (International Association for the Properties of Water and Steam) reference EoS for pure water (H_2O) [22], while Span and Wagner [23] were able to generate the most accurate EoS for carbon dioxide (CO_2). Handling such fundamental equations often proves to be rather laborious since separate and large sets of constants have to be considered for each subregion that the global range in a V - T plane or a P - T plane is divided into. Crossing the border between two neighboring subregions requires special subroutines for a smooth transition.

The people around Wagner and Span later came up with several sophisticated Helmholtz energy-based fundamental EoSs for heavy water, chlorine, and monoethanolamine [24, 25] as well as for liquefied natural gases (LNG). These latest EoSs even cover many CO_2 -rich mixtures relevant for CCS (CO_2 capture and storage) and others. What remains is the fact that the numerous coefficients for these highly sophisticated equations cannot be determined without appropriate sets of experimental data because the former are no longer unambiguous representations of physical interactions between molecules. Hence, it comes as no surprise that one of the early cubic equations could be

extended into a coherent framework, the so-called PSRK (predictive Soave-Redlich-Kwong EoS) [26], for the calculation of phase equilibria of binary mixtures even in cases when there are no experimental data available. Here, the attractive and the repulsive terms, a and b , of a mixture are calculated applying a mixing rule to pure-compound parameters in which the non-ideality of the mixture is accounted for by a g^E term from a group contribution algorithm that is borrowed from or similar to the UNIFAC theory for low-pressure mixtures.

2 Thermodynamic Calculations

Most of the EoSs are given in their pressure-explicit form so that the pressure P can be calculated in one single step for any given set of V and T . Holding T constant and varying V from infinity downwards to the lowest values that are still realistic for a condensed fluid, isotherms can be plotted onto a P - V plane. Subcritical isotherms, i.e., those for $T < T_c$ will exhibit one relative minimum for the pressure, $P_{\min}(T)$, and one relative maximum, $P_{\max}(T)$, featuring an inflexion point between them. These three loci will coincide into P_c on a critical isotherm, where $T = T_c$. On every supercritical isotherm, there will be an inflexion point but neither a relative minimum nor a relative maximum. Since for many engineering applications it is more desirable to determine the density ρ of a fluid as a function of P and T , an inverse algorithm is needed. At supercritical temperatures, all isotherms have exactly one positive and finite root for V as long as P and T are also positive and finite. The required density ρ is defined as the inverse value of V , i.e., $\rho = 1/V$. For all subcritical isotherms, the saturation pressure P^s must be found first within the range $P_{\min}(T) < P^s(T) < P_{\max}(T)$ and satisfying the Maxwell criterion (Eq. (11)).

$$P^s(T) = \frac{1}{V_g - V_l} \int_{V_l}^{V_g} P(T, V) dV \quad (11)$$

Thus, for a given subcritical temperature T , a positive pressure $P > P^s(T)$ will always yield one or several real roots for V , out of which the smallest value, V_l , represents the fluid at its only stable density at P and T (the remaining roots representing metastable or unstable states, respectively) indicating a liquid phase. Pressures below the saturation pressure, $P < P^s(T)$, also yield one or several real roots for V , out of which the largest value, V_g , represents the only stable state, this time being a gaseous phase. When the pressure P coincides with the saturation pressure of a given temperature, two of the various real roots for V , i.e., V_g and V_l , represent stable states marking the boundary of the two-phase region in a P - V plane. The respective densities, $\rho_l = 1/V_l$ and $\rho_g = 1/V_g$, of the two co-existing phases are readily determined. This implies that the factual density of a pure fluid at T and $P = P^s(T)$ will range from ρ_g to ρ_l depending

on the mass fraction of either phase. Determining the saturation pressure $P^s(T)$ together with the specific volumes of the two co-existing phases, V_l and V_g , over a sufficiently wide range of subcritical temperatures results in a binodal curve on a P - V plane and in a vapor pressure function on a P - T plane.

In a rather generalized way, cubic EoSs could be conceived as having the following format, in which $\alpha(T)$ (later $\alpha(T, \omega)$) is a correction term by which the temperature dependence of the attractive term, a , is taken into account, and where u and v are natural numbers ranging between 0 and 2 (see Tab. 1):

$$P = \frac{RT}{V-b} - \frac{\alpha(T)a}{V^2 + ubV + wb^2} \quad (12)$$

The earliest cubic EoSs were traditionally entered by not more than two fluid-specific constants, which were computed from P_c and T_c in most cases. By design, this results in a vapor pressure function that ends exactly at P_c and T_c , while neither the saturation pressure $P^s(T < T_c)$ predicted for subcritical temperatures nor the respective densities of the co-existing fluid phases necessarily agree too well with experimental values. Cubic EoSs traditionally work reasonably well for the prediction of the densities of the gaseous phase but are less successful at predicting the critical compressibility and fluid densities of the liquid phase.

Introducing the acentric factor according to Pitzer, ω , as a third fluid-specific constant [13] by Eq. (13), led to very powerful improvements. Its implementation makes it possible to skew the vapor pressure function generated by a cubic EoS and, therefore, to fit it much better to experimental values.

$$\omega = -\log\left(P_{r(T_r=0.7)}^s\right) - 1 \quad (13)$$

Altering the polynomial structure of a cubic EoS can contribute to a closer agreement between Z_c as predicted by the EoS and experimental values.

Eq. (14) is the EoS as composed of a hard-sphere term according to Carnahan and Starling [14] and an attractive term analogous to the Redlich-Kwong EoS taken from [15] and reads

$$P = \frac{RT}{V} \left[1 + \frac{4\eta - 2\eta^2}{(1-\eta)^3} \right] - \frac{a}{\sqrt{T}V(V+b)} = \frac{RT}{V} \left[\frac{1 + \frac{b}{4V} + \left(\frac{b}{4V}\right)^2 - \left(\frac{b}{4V}\right)^3}{\left(1 - \frac{b}{4V}\right)^3} \right] - \frac{a}{\sqrt{T}V(V+b)} \quad (14)$$

As with cubic EoSs, the effect of these structural modifications on Z_c is widely independent of the skewing of the vapor pressure function effectuated by Pitzer's factor ω . This independence is given up on in Eqs. (7) and (8) by Platzer and Maurer as well as in Eqs. (9) and (10) of Lee and Kesler, where changes in ω are always accompanied by changes in Z_c . However, this connection between Z_c and ω is supported by experimental data. When ω is conceived as a measure for the sphericity of a molecule, then, there appears to be a somewhat surprising connection between the shape of a molecule, the slope of its vapor pressure function, and its critical compressibility, Z_c . This applies quite well to nonpolar fluids as is shown in Fig. 2.

Since an overwhelming majority of $Z = Z(P_r, T_r)$ diagrams published for the Lee-Kesler EoS are generated with $\omega = 0$ and, hence, $Z_c = 0.2905$, we deem it worthwhile to mention that the one locus on an isotherm where $(\partial P/\partial V)_T = 0 = (\partial^2 P/\partial V^2)_T$ is obtained for a reduced temperature of $T_r = 1 + \varepsilon_T \omega$ approximately, resulting in a reduced pressure $P_r = 1 + \varepsilon_P \omega$ for $-0.4 \leq \omega \leq 0.25$. It was found that $\varepsilon_T = -0.035$ and $\varepsilon_P = -0.08$.

The generalized Bender EoS of Platzer and Maurer contains an additional fluid-specific variable, χ , that similarly

Table 1. The development and improvement of cubic EoSs over the course of one century [21].

Equation of state	u	w	$\frac{bP_c}{RT_c}$	$\frac{aP_c}{R^2T_c^2}$	$\alpha(T)$	Z_c
van der Waals	0	0	1/8 = 0.125	27/64 = 0.421875	1	3/8 = 0.375
Redlich-Kwong	1	0	0.08664	0.42748 $\sqrt{T_c}$	$T^{-1/2}$	1/3 = 0.333
Soave-Redlich-Kwong	1	0	0.08664	0.42747	$\left[1 + \kappa(\omega) \left(1 - \sqrt{\frac{T}{T_c}} \right) \right]^2$, wherein $\kappa(\omega) = 0.48505 + 1.55171\omega - 0.15613\omega^2$	1/3 = 0.333
Peng-Robinson	2	-1	0.077796	0.457235	$\left[1 + \kappa(\omega) \left(1 - \sqrt{\frac{T}{T_c}} \right) \right]^2$, wherein $\kappa(\omega) = 0.37464 + 1.54226\omega - 0.26992\omega^2$	0.3074
Carnahan-Starling-Redlich-Kwong	1	0	0.1050	0.4619 $\sqrt{T_c}$	$T^{-1/2}$	0.316

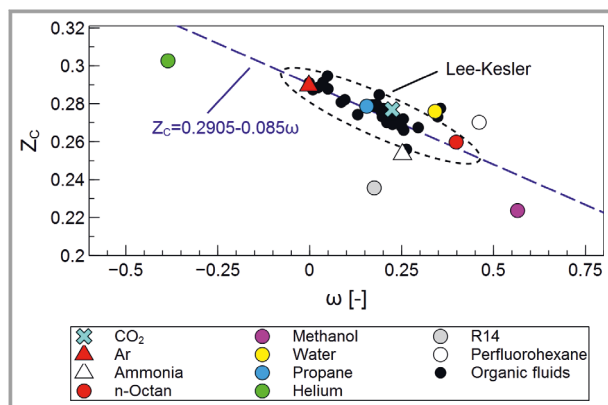


Figure 2. The critical compressibility Z_c vs the acentric factor ω of eleven different fluids. Strong correlation for nonpolar fluids that are well represented by the EoS of Lee and Kesler (Eqs. (9) and (10)) where there is a systematic dependence of the nature $Z_c = 0.2905 - 0.085\omega$ (Herrig [25]).

skews – or un-skews – the vapor pressure function while leaving Z_c untouched. Halm and Stiel [27] had introduced this factor as an additional parameter to describe the behavior of polar fluids. χ can be calculated [20] using Eq. (15) whereby ω and the reduced vapor pressure $P_r(T_r = 0.6)$ at the temperature $T = 0.6T_c$ of the fluid need to be known.

$$\chi = \log\left(P_{r(T_r=0.6)}^s\right) + 1.7\omega + 1.552 \quad (15)$$

Fig. 3 shows which values of ω and χ apply best for a variety of fluids, and how, with the EoS of Lee and Kesler, the polar factor χ cannot be varied independently from ω , or not at all, that is.

The MPEoSs treated so far, e.g., Eqs. (7)–(10), are purely volumetric, which makes them apparently insufficient whenever caloric variables of state are required. However, combining them with just one basic caloric EoS will provide for all of the additional capabilities. C_p^{IG} is the ideal-gas spe-

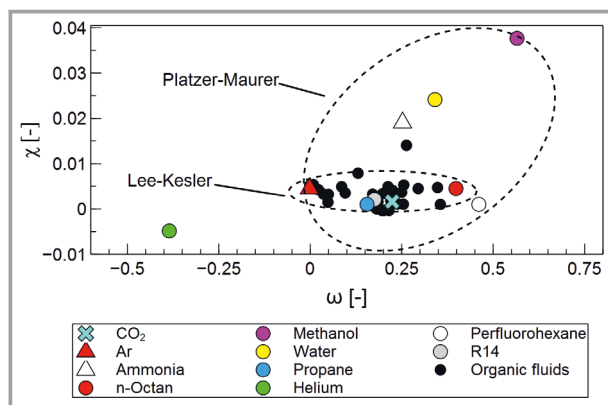


Figure 3. Polar factor χ and acentric factor ω as they are drawn from the saturation pressure functions of various fluids by Eqs. (13) and (15). Areas covered by the Lee-Kesler EoS (Eqs. (9) and (10)) and by the Platzer-Maurer EoS (Eqs. (7) and (8)) are encircled.

cific heat capacity and as such only depending on the temperature. Eq. (16) gives a polynomial expression for $C_p^{IG}(T)$, wherein a , b , c , and d are given as a set of constants that are available from tables for many pure species. While second-order or third-order polynomials are most common, higher polynomials with positive and integer exponents are available (especially for extended temperature ranges) and some even contain a T^{-2} term or an exponential term as in Einstein's heat capacity for solids.

$$C_p^{IG} = a + bT + cT^2 + dT^3 \quad (16)$$

Relying on Eq. (16), the specific inner energy, $U(V,T)$, and the specific enthalpy of a fluid, $H(V,T)$, can be readily calculated using Eqs. (17) and (18). Note that $U(V,T) = H(V,T) - PV$.

$$H(V, T) = H^{IG}(T) + \int_{\infty}^V \left[T \left(\frac{\partial P(T, V)}{\partial T} \right)_V - P(T, V) \right] dV + PV - RT \quad (17)$$

wherein

$$H^{IG}(T) = H_0^{IG} + \int_{T_0}^T C_p^{IG}(T) dT \quad (18)$$

In this work, Eq. (17) is used to calculate the specific enthalpy of evaporation as shown in Eq. (19).

$$\Delta H_{\text{vap}} = H(V_g, T) - H(V_l, T) = T \int_{V_l}^{V_g} \left(\frac{\partial P(V, T)}{\partial T} \right)_V dV \quad (19)$$

The speed of sound, c_{snd} , is computed using Eq. (20).

$$c_{\text{snd}}^2(V, T) = \left(\frac{\partial P(V, T)}{\partial \rho} \right)_s = -V^2 \frac{C_p}{C_v} \left(\frac{\partial P(V, T)}{\partial V} \right)_T \quad (20)$$

whereby the values of $C_p^{IG}(T)$, C_v , and C_p need to be determined with Eqs. (16), (21), and (22).

$$C_v(V, T) = C_p^{IG}(T) - R + T \int_{\infty}^V \left[\left(\frac{\partial^2 P(V, T)}{\partial T^2} \right)_V \right] dV \quad (21)$$

$$C_p(V, T) = C_v(V, T) - T \left(\frac{\partial P(V, T)}{\partial T} \right)_V^2 \left(\frac{\partial P(V, T)}{\partial V} \right)_T^{-1} \quad (22)$$

Properties of one specific fluid as obtained from a given EoS can be held in comparison to “true” reference values originating from the most accurate EoS available for that fluid. There is or has been a certain competition going on

for the formulation of the most accurate and most reliable reference EoSs for various fluids. The reference equations are fundamental EoSs in most cases and, as such, each based on a large number of specific constants. They commonly express either the specific Helmholtz energy, $F(T,\rho)(RT)^{-1} = \Phi(\tau,\delta)$, or the specific Gibbs enthalpy, $G(P,T)(RT)^{-1} = \Gamma(\pi,\tau)$ as dimensionless functions of dimensionless variables of state such as the temperature, τ , the density, δ , and the pressure, π . The respective constants are obtained through very laborious and sophisticated parameter fitting procedures aiming at the best fit for a carefully selected set of experimental data obtained from measurements of, e.g., the speed of sound or other higher derivatives. In this paper, we refer to standard values for comparison that are obtained from a fundamental EoS for water, IAPWS-IF97, by Wagner and Kruse [22], from another fundamental EoS for carbon dioxide by Span and Wagner [23], and from a software package for pure helium (He), HEPAK [28], which itself is a refinement of a fundamental EoS developed by McCarty [29].

The critical data of water, carbon dioxide, and helium are compiled in Tab. 2 along with the molar mass, the acentric factor, ω , the polar factor, χ , and four coefficients for the ideal-gas heat capacity of said species. Some or all of these data enter various cubic EoSs and MPEoSs that have been introduced in the sections above. All of the EoSs from which the results are shown and compared in the following sections are well established and can be found in the literature, e.g., [21] and [30].

Table 2. Critical and other data of water, carbon dioxide, and helium, as required for the volumetric part and for the calorific part of various EoSs.

Parameter	Water	Carbon dioxide	Helium
Critical temperature T_c [K]	647.096	304.128	5.15953
Critical pressure P_c [MPa]	22.064	7.3773	0.22746
Critical volume V_c [cm ³ mol ⁻¹]	55.948	94.118	57.4746
Molecular mass M [g mol ⁻¹]	18.015	44.0098	4.0026
Acentric factor ω [-]	0.34437	0.22394	-0.3854
Polar factor $\chi \cdot 10^3$ [-]	23.6065	1.626	4.8656
Heat capacity, $C_p^{\text{IG}}(T) = C_p^0(T)$			
Coefficient a [J mol ⁻¹ K ⁻¹]	32.218	19.78	5/2R
Coefficient b [10 ⁻³ J mol ⁻¹ K ⁻²]	1.91	73.39	-
Coefficient c [10 ⁻⁶ J mol ⁻¹ K ⁻³]	10.55	-55.98	-
Coefficient d [10 ⁻⁹ J mol ⁻¹ K ⁻⁴]	-3.593	17.14	-

2.1 Practical Statement for the Use of EoSs while Computing Thermodynamic Properties

When practically dealing with engineering problems where thermodynamic properties of at least one fluid are needed to perform higher-order calculations, scientists and engineers have a plethora of options where to obtain reliable data, software packages, or even universally applicable subroutines as DLL files or extensions for their spread-sheet programs. Among many others, some of the most distinguished platforms include: NIST with its REFPROP package, the process simulation software ASPEN PLUS, IK-CAPE of DETHERM, the TREND package (under development) of Ruhr-Universität Bochum, which all are commercial products and, therefore, more or less expensive. As an alternative, the basis version of FluidProp is a free download.

3 Results and Discussion

3.1 Using State-of-the-Art EoSs as Reference

In this paper, the results obtained from a variety of rather original or simple EoSs are compared to those considered state of the art. Thus, the question might arise why the calculated data are not compared to measurements. Measuring thermodynamic data of a fluid accurately is an art in and on itself, sometimes mastered by the same scientists who brought up one of the EoSs used as a reference here. The accuracy of these equations often lies within the confidence interval of the measurements. In the following paragraphs, some light will be shed on the accuracy of each of the EoSs used as a reference here.

3.1.1 Reference for Water (IAPWS-97)

The detailed accuracy of the calculated values is discussed in [32] and [33] for all regions. However, in conclusion, it shows that vapor pressures $\Delta P^s/P^s$ can be found within 0.02 and 0.05 % accuracy. The specific volume $\Delta V/V$ can be found within 0.003 and 0.015 % for the liquid phase, within 0.05 and 0.15 % for the gaseous phase (0.3 % for $T > 800$ K and $P > 4$ MPa), and within 0.2 % near the critical point. The absolute uncertainties in the enthalpy of evaporation $\Delta(\Delta H_{\text{vap}})$ are 0.5 kJ kg⁻¹ for $T < 620$ K, 4 kJ kg⁻¹ for $T < 644$ K, and > 8 kJ kg⁻¹ for $T = 644$ K up to $T_c = 647.096$ K. The speed of sound can be calculated for the most of the ranges with an accuracy of 0.3 %. However, near the critical point the values are 0.5 % and for $T \geq T_c$ and $P > 10$ MPa up to 1 %.

3.1.2 Reference for Carbon Dioxide

For carbon dioxide the fundamental EoS by Span and Wagner is used. It contains also several sets of parameters for different regions. The EoS and its accuracy is discussed in [23]. It is shown that the vapor pressure $\Delta P^s/P^s$ can be

found within 0.01 % accuracy. The volumetric uncertainties $\Delta\rho/\rho$ in the PVT surface are considered 0.03 % for $T < 375$ and $P < 10$ MPa, 0.05 % for $T > 375$ and $P < 20$ MPa, and up to 1–2 % for $P > 20$ MPa. The accuracy of the caloric properties is discussed using measurement data from C_p . For the saturation line, the accuracy ΔC_p is considered within 1–1.5 % for $T < 295$ K and 2 % for $T = 295$ K - $T_c = 304.1282$ K. The speed of sound in the fluid phase can be calculated within 2 % and in the gas phase 0.5 % for $T < 301$ and 3 % for $T > 301 - T_c$.

3.1.3 Reference for Helium

The reference EoS for helium is implicated in the computer program HEPAK for calculating properties from the melting line up to 1500 K. The details are presented in [28]. The accuracy statement of the program is summarized for densities as 0.2–0.5 %, enthalpies and other caloric properties within 2 and 3 %, and the speed of sound can be calculated within 0.1 %.

3.2 Vapor Pressure

When solving the Clausius-Clapeyron relation for the phase change of a real fluid and under some simplifying assumptions, a very basic vapor pressure correlation can be obtained, which is sometimes referred to as the August equation (Eq. (23)), where A and B are specific constants (not to be confounded with some of the constants introduced earlier).

$$\log_{10}(P^s) = A - \frac{B}{T} \quad (23)$$

From this correlation, any saturation pressure function is expected to be a straight line when being plotted in a P - T plane, where the P -axis has a logarithmic scale while the marks on the T -axis scale with the inverse value of T .

We used the correlation derived from the EoS by Lee and Kesler (Eqs. (9) and (10)) to illustrate how well this idealized expression approximates rather realistic vapor pressure correlations. And we show how the acentric factor according to Pitzer affects the slope of the resulting curves in Fig. 4a.

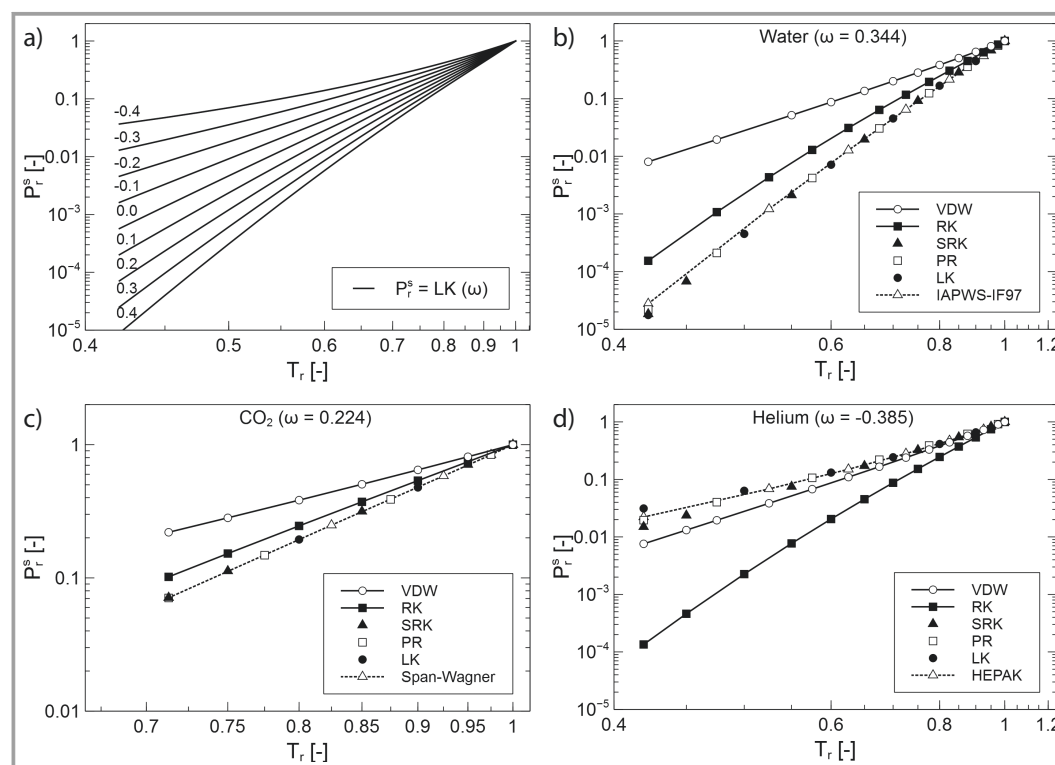


Figure 4. a) Reduced vapor pressure P_r^s as obtained from the Lee-Kesler EoS and as a function of both the reduced temperature T_r and the acentric factor according to Pitzer, ω . It can be seen that, for $\omega = 0$, the vapor pressure at $T_r = 0.7$ is $P^s(T = 0.7T_c) = 0.1P_c$. b) Reduced vapor pressure P_r^s of water as a function of the reduced temperature T_r . The results obtained from five different EoSs, authored by van der Waals (VdW), Redlich-Kwong (RK), Soave-Redlich-Kwong (SRK), Peng-Robinson (PR), and Lee-Kesler (LK), can be compared to the reference values computed using the fundamental EoS IAPWS-IF97 by Wagner and Kruse. c) Reduced vapor pressure P_r^s of carbon dioxide as a function of the reduced temperature T_r . The results obtained from five different EoSs can be compared to the reference values computed using the fundamental EoS by Span and Wagner. d) Reduced vapor pressure P_r^s of helium as a function of the reduced temperature T_r . The results obtained from five different EoSs can be compared to the reference values computed using the software package HEPAK.

The vapor pressure $P_r^s = P^s/P_c$ function according to Lee-Kesler is:

$$\ln(P_r^s) = f^{(0)} + \omega f^{(r)} \quad (24)$$

wherein

$$f^{(0)} = 5.92714 - \frac{6.09648}{T_r} - 1.28862 \ln(T_r) + 0.169347 T_r^6 \quad (25)$$

$$f^{(r)} = 15.2518 - \frac{15.6875}{T_r} - 13.4721 \ln(T_r) + 0.435777 T_r^6 \quad (26)$$

Figs. 4b–d show reduced vapor pressures as obtained from various EoSs for water, carbon dioxide, and helium. With some of the EoSs employed here, the Maxwell criterion (Eq. (11)) had to be satisfied to solve for $P_r^s = P^s(T_r)$. Two of the cubic EoSs that are not entered by the acentric factor according to Pitzer in any way, i.e., the VdW EoS (Eq. (3)) and the RK EoS [31], invariably produce vapor pressure functions corresponding to those where this factor is otherwise set to $\omega = -0.302$ (VdW), or $\omega = 0.059$ (RK), respectively. This shows how much of an improvement it was when early EoSs were made to account for a temperature dependence of the attractive term in a way that required not more than one additional parameter. Vapor pressures predicted by EoSs, such as SRK, PR, or LK, are in remarkably close agreement with results from the respective reference EoS.

Calculating the reduced vapor pressure, P_r^s , can be done using the critical data of one specific fluid to determine $P^s(T)$ as explained in previous sections followed by normalizing $P^s(T)$ by P_c and T by T_c of the same fluid. Alternatively, P_r^s can be found through a universal procedure independent of the peculiarities of any specific fluid. As an example, a normalized EoS according to Peng and Robinson is given:

$$P_r(V_r, T_r) = \frac{P(V, T)}{P_c} = \frac{T_r}{(V_r - b_r)} - \frac{\alpha(\omega, T) a_r}{(V_r^2 + 2b_r V_r - b_r^2)} \quad (27)$$

wherein the expressions $a_r = aP_c/(R^2 T_c^2) = 0.457235$, $b_r = bP_c/(RT_c) = 0.077796$, and $V_r = VP_c/(RT_c)$ are dimensionless as well. For a given T_r , P_r is varied until the dimensionless specific volumes for the liquid phase and the gaseous phase, $V_{r, \text{liq}}(P_r, T_r)$ and $V_{r, \text{gas}}(P_r, T_r)$ in combination with said P_r meet the dimensionless Maxwell criterion.

$$P_r^s(V_{r, \text{gas}} - V_{r, \text{liq}}) = \int_{V_{r, \text{liq}}}^{V_{r, \text{gas}}} P_r(V_r, T_r) dV_r \quad (28)$$

3.3 Volumetric Properties

Once the vapor pressure of a given fluid at any subcritical temperature has been determined properly, the picture of its volumetric properties, e.g., density, can be completed. While its density can be calculated in a P - T range that encompasses the two-phase region, a binodal line can be plotted on a P - V plane separating the single-phase region from the two-phase region. On that same plot, subcritical real-gas isotherms will cross the two-phase region horizontally.

Plotting isotherms on a P - V plane did, however, not appear to us to be the best method to illustrate how choosing a specific EoS, or changes, e.g., in ω affect the densities of either phase. Therefore, we present one Z - P plot, and three different ρ - T plots in this subsection.

As shown in Fig. 5a, increasing ω leads to lower vapor pressures at any given subcritical temperature as well as to a lower critical compressibility, and, while it increases the fluid densities at saturation conditions, it produces lower densities at supercritical conditions.

Figs. 5b–d illustrate the difficulties that are involved when using various EoSs to predict the densities of a fluid at saturation conditions. For water, the density of the liquid phase at saturation conditions is best represented by IAPWS-IF97 and is generally underpredicted by virtually all other EoSs. The deviations from the reference values range from more than 40% to less than 1% as one proceeds from the EoSs of van der Waals, Redlich-Kwong, and Peng-Robinson to the ones of Lee-Kesler, Bender, and Platzler and Maurer. This picture is similar but yet different when describing the liquid density of carbon dioxide. Here, the reference values given by the EoS of Span and Wagner can be satisfactorily approximated by most of the EoSs. They are, however, considerably underestimated by the EoS taken from Redlich-Kwong as well as Soave-Redlich-Kwong and even more so by the van der Waals EoS. The whole situation looks very different for helium, where $\omega = -0.3854$. Here, the reference densities obtained from HEPAK are remarkably well approximated by the EoS of van der Waals. This is less surprising when we are reminded that van der Waals was explicitly concerned with the volumetric properties of helium and that his original EoS always produces saturation conditions at $T_r = 0.7$ that correspond to $\omega = -0.302$. This can explain in part why the liquid densities of helium are overpredicted by almost all general EoSs. The results from the EoS by McCarty are the only ones virtually indiscernible from the reference values.

3.4 Heat of Evaporation

The enthalpy of evaporation of a specific fluid, ΔH_{vap} , as it depends on temperature or pressure, is an important parameter in many processes. Therefore, accurate numerical values of it are crucial for process simulations. Figs. 6, 7, and 8 show the dimensionless heat of vaporization,

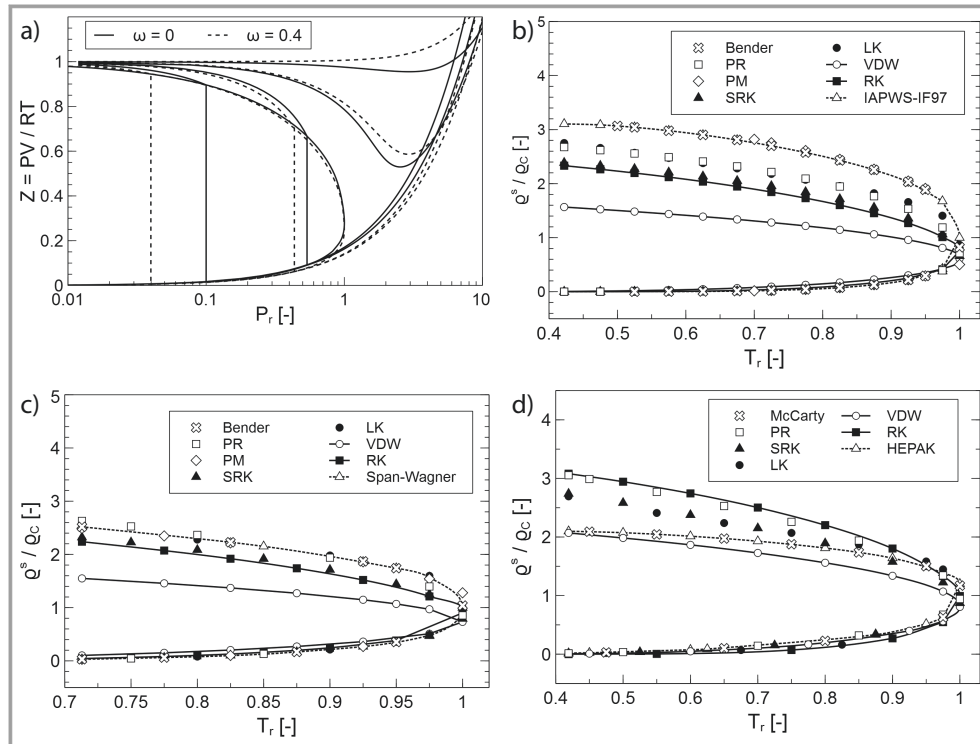


Figure 5. a) Compressibility factor Z obtained from the Lee-Kesler EoS, and plotted as a function of the reduced pressure, P_r , while the reduced temperature T_r is held constant at five representative values ($T_r = 0.7, 0.9, 1.0, 1.2,$ and 2.0). The isotherms and the binodal line are shown for two different values of ω . b)–d) Reduced density, ρ^s/ρ_c , of water, carbon dioxide, and helium at saturation conditions and as a function of the reduced temperature. Results are shown for EoSs authored by VdW, RK, SRK, PR, LK, Platzler and Maurer (PM), and by Bender or McCarty. Reference data were obtained from IAPWS-IF97 (H_2O), the fundamental EoS by Span and Wagner (CO_2), and from the software package HEPAK (He).

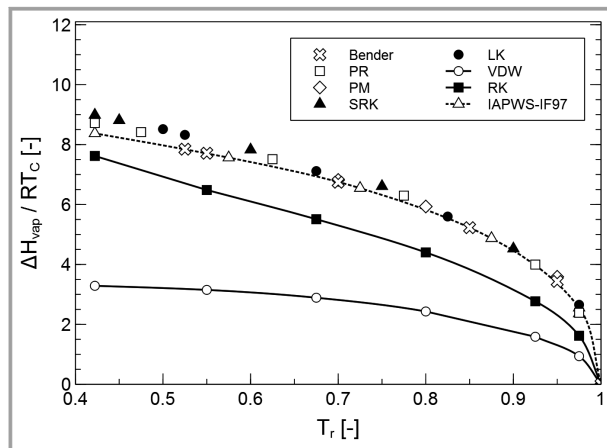


Figure 6. Dimensionless enthalpy of evaporation of water as a function of the reduced temperature, calculated using seven different EoSs authored by VdW, RK, SRK, PR, LK, PM, and by Bender. Reference values have been computed using the EoS IAPWS-IF97.

$\Delta H_{vap}/(RT_c)$, computed from various EoSs for water, CO_2 , and helium as functions of the reduced temperature T_r .

As has been shown in previous sections, an accurate calculation of the heat of vaporization is closely related to the

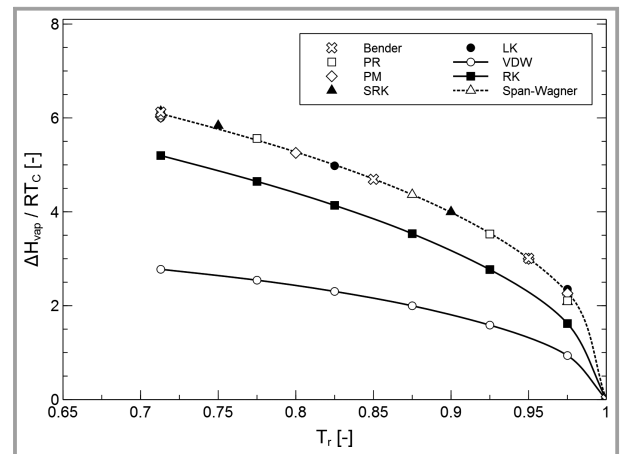


Figure 7. Dimensionless enthalpy of evaporation of carbon dioxide as a function of the reduced temperature, calculated using seven different EoSs. Reference values have been computed using the EoS of Span and Wagner.

accuracy of the results obtained for the saturation pressure as well as for the fluid densities of either phase at saturation conditions. While deviations in gas-phase density can have a considerable impact on the resulting heat of vaporization,

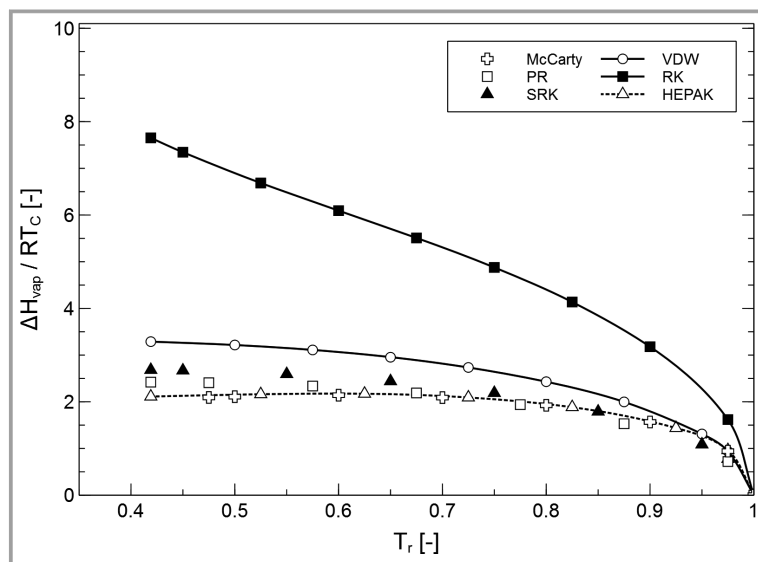


Figure 8. Dimensionless enthalpy of evaporation of helium as a function of the reduced temperature, calculated using five different EoSs. Reference values have been computed using the software package HEPAK.

those on the liquid side of the binodal line will not. This is why, for water and CO_2 , virtually all of the EoSs deliver reasonable results throughout the whole temperature range, the two exceptions being the EoS of van der Waals and the one by Redlich-Kwong. This picture is, again, a little bit different when the heat of vaporization of helium is to be calculated. The EoS of Redlich-Kwong is off by a factor of up to 4. The EoS of van der Waals delivers surprisingly reasonable results as its predictions are off by a margin no larger than some 50%. The results of all other EoSs lie within an error margin of 10–20% (PR EoS, SRK EoS) or better.

3.5 Speed of Sound

Delivering accurate values for the speed of sound, c_{snd} , as defined in Eq. (20) and over a wide range of pressures and temperatures is a meaningful criterion when the usefulness and reliability of an EoS must be judged. Especially in the near-critical region, where the density of the fluid changes most dramatically, there is an elevated risk for higher inaccuracies with most common EoSs.

This is illustrated by Fig. 11a, where results obtained from the Redlich-Kwong EoS for pure helium are compared to reference values from HEPAK.

In the following paragraphs, contour plots of the error margins as they appear in a P - T plane when the speed of sound is calculated using different types of EoSs will be presented and, subsequently, compared to the respective reference values. Some diagrams exhibit what may look like an inaccessible region enclosed by the respective vapor pressure functions of the reference EoS and the EoS under scrutiny.

3.5.1 Water

It is clearly illustrated by Figs. 9a–d that none of the cubic EoSs can produce reliable values for the speed of sound in the near-critical or in the pseudo-critical region. The contour plots of the van der Waals EoS, the Soave-Redlich-Kwong EoS, and the Peng-Robinson EoS are similar in shape and quantitatively comparable. Fig. 9d substantiates the claim of marked improvement that is achieved by a MPEoS, here the Bender EoS.

3.5.2 Carbon Dioxide

For carbon dioxide, the results obtained from various EoSs were compared to reference data calculated by use of the EoS of Span and Wagner. Here again, while the Soave-Redlich-Kwong EoS (Fig. 10b) and the Peng-Robinson EoS (Fig. 10c) show considerable improvement in accuracy over the van der Waals EoS (Fig. 10a), all three of them produce, as cubic EoSs, unsatisfactory results, partly in the pseudo-critical region and especially in the near-critical region. This sobering picture is superseded by a drastically improved accuracy (Fig. 10d) once a MPEoS such as the Bender EoS is invoked.

3.5.3 Helium

For helium, the results obtained from various EoSs were compared to reference data calculated by use of the software package HEPAK. As Fig. 11b shows, predictions of the speed of sound by the van der Waals EoS grow from well acceptable at supercritical temperatures and subcritical pressures to inaccurate as soon as the pressure is supercritical too, and finally, to problematic as the temperature is shifted to subcritical values at supercritical pressures. Fig. 11c shows that these problems are significantly reduced by the Soave-Redlich-Kwong EoS, where inaccuracies at subcritical pressures are still considerable. Finally, the deviations between the standard values by HEPAK and the EoS by McCarty (Fig. 11d) are rather purely numerical in nature as the equations under HEPAK strongly draw on the original EoS by McCarty.

3.6 Practical Application: Designing Safety Valves for Near-Critical Helium Using EoSs

A concluding illustration can be obtained when an adiabatic expansion of supercritical helium into the near-critical or pseudo-critical region is simulated using various EoSs. Here, the frictional effects are summarily taken into account by a factor r_f as defined in Eq. (29).

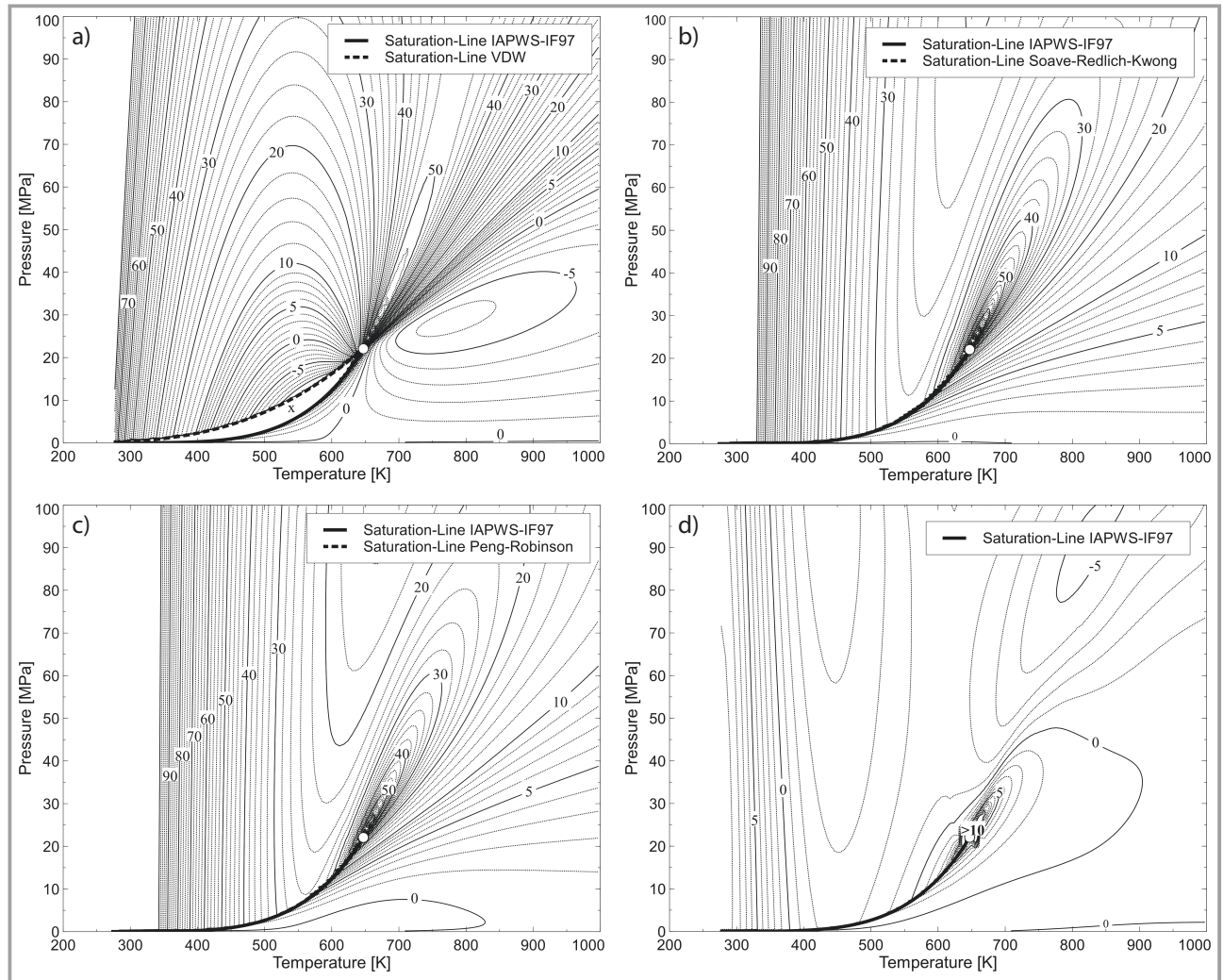


Figure 9. Error margins in % deviation resulting from the computation of the speed of sound of water when using a) the van der Waals EoS, b) the Soave-Redlich-Kwong EoS, c) the Peng-Robinson EoS, and d) the Bender EoS to solve Eq. (20). The primary results were held against reference values generated with the IAPWS-IF97 EoS of Wagner and Kruse.

$$r_f = \frac{dW_{diss}}{-VdP} \Rightarrow r_f = \frac{W_{diss,12}}{-W_{t,12}^{rev}} \quad (29)$$

An expansion that is affected by friction in this way, will evolve in a P - V diagram along a path given by Eq. (30).

$$-\frac{dT}{dV} = \left(\frac{\partial P}{\partial V}\right)_T \left\{ \left(\frac{\partial P}{\partial T}\right)_V - \frac{C_p(V, T) \frac{1}{T}}{\left[\left(\frac{\partial V}{\partial T}\right)_P - r_f \frac{V}{T}\right]} \right\}^{-1} \quad (30)$$

As long as $0 < r_f < 1$, acceleration of the gas is a premier consequence of its expanding next to the pressure drop. For the gas velocity c , we have Eqs. (31) and (32).

$$d\left(\frac{1}{2}c^2\right) = cdc = (1 - r_f) \frac{V}{M} (-dP) \quad (31)$$

$$\Rightarrow c_2 = \sqrt{c_1^2 - \frac{2(1 - r_f)}{M} \int_{P_1}^{P_2} V(P, T) dP} \quad (32)$$

Eqs. (30)–(32) in combination with $P = P(V, T)$ have been solved numerically for a flow process in which helium is expanded adiabatically from stagnation conditions at $P_0 = 23$ bar and $T_0 = 10$ K first to $P_1 = 11$ bar and later to choked and sonic conditions, where $c_3 = c_{snd}(V_3, T_3)$. Combining the data obtained from those computations for the flow speed and the density allows for the calculation of a specific mass flux, \dot{m}_i , at any cross section of a fictitious straight channel in which the expanding gas is flowing. Referring to the design of a safety valve, the theoretical maximum lifting force per unit area of the cross-section,

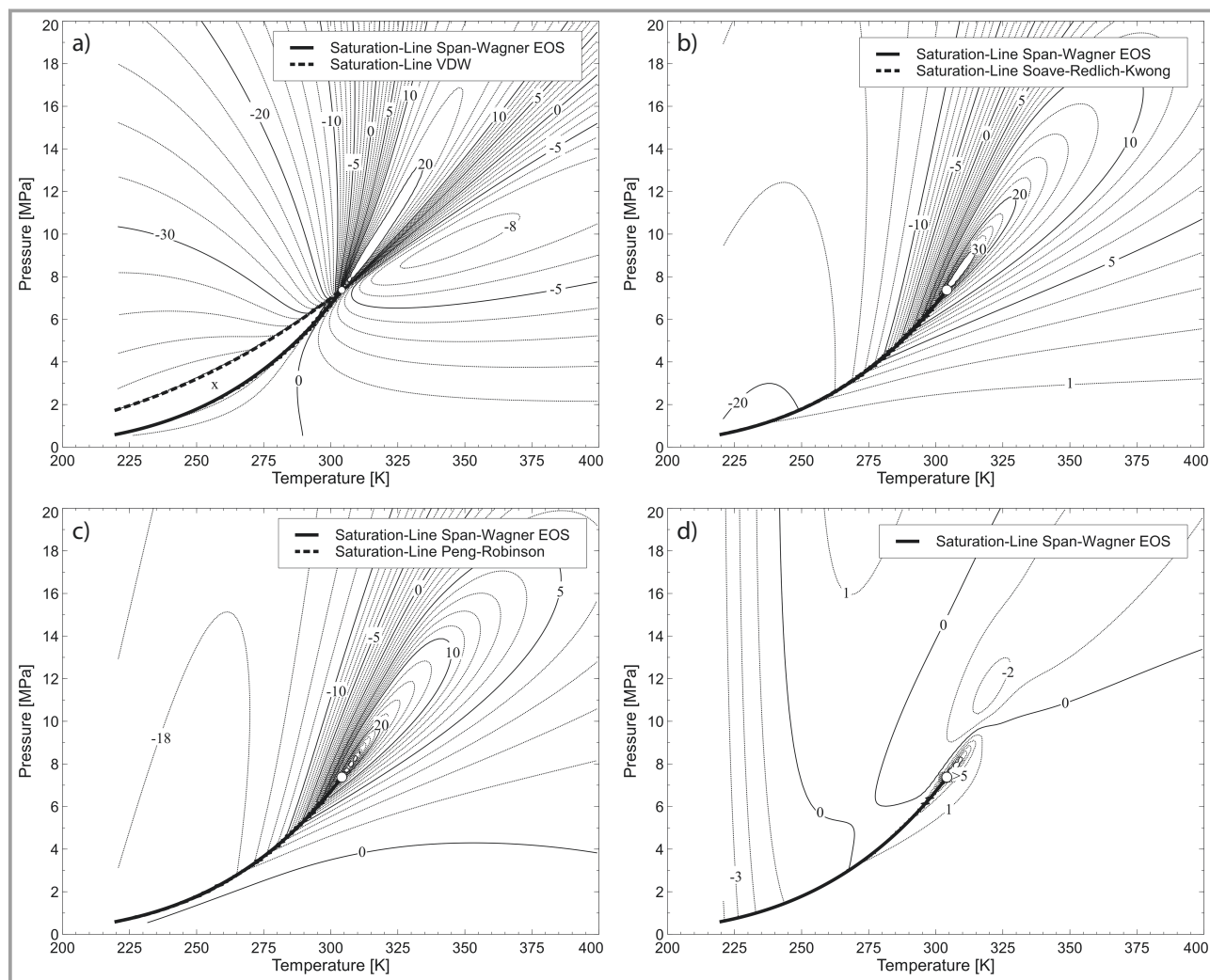


Figure 10. Error margins in % deviation resulting from the computation of the speed of sound of carbon dioxide when using a) the van der Waals EoS, b) the Soave-Redlich-Kwong EoS, c) the Peng-Robinson EoS, or d) the Bender EoS to solve Eq. (20). The primary results were held against reference values generated with the EoS of Span and Wagner.

f_{i3}^* , can be obtained from the reversal of the momentum flux.

The numerical results for a frictionless expansion can be found in Tab. S1 in the Supporting Information, while those for a frictional expansion with $r_f = 0.3$ and $r_f = 0.5$ are given in Tabs. S2 and S3, respectively. They were obtained by eight different EoSs and are compared to results from HEPAK as well as to those obtained for air using the ideal gas law. Reference Reynolds numbers, mass flow rates, and reaction forces upon momentum flux reversal are given for a circular cross section with $D = 30$ mm.

It is striking how predictions of the specific volume as obtained by various EoSs show larger deviations from the reference value given by HEPAK than the flow velocities, the specific mass flow rates, and the maximum reaction forces.

From the corresponding diagrams in Figs. 12, 13, and 14 it can be recognized that EoSs operating properly with an

acentric factor according to Pitzer are categorically superior to all others, which in this case includes the EoS of Platzer and Maurer since the latter cannot account for negative values of ω . It is remarkable, albeit perhaps not too surprising, that the EoS of Soave, Redlich, and Kwong outperforms not only the EoS of van der Waals but also the ones by Peng and Robinson and by Lee and Kesler – the latter even by a larger margin. For this rather unexpected “underachievement” of the Lee-Kesler EoS, the following reason is suggested: while it correlates the critical compressibility, Z_c , with the acentric factor according to Pitzer, ω , qualitatively correctly, i.e., it exhibits a decreasing Z_c with increasing ω (see Fig. 2), it overestimates the critical compressibility of helium at around $Z_c = 0.32$, while the correct value for $\omega = -0.3854$ as valid for helium would have been $Z_c = 0.305$. This overprediction is correlated to a systematic underprediction of liquid-phase densities. The fact that the SRK EoS outperforms the PR EoS might be related to the

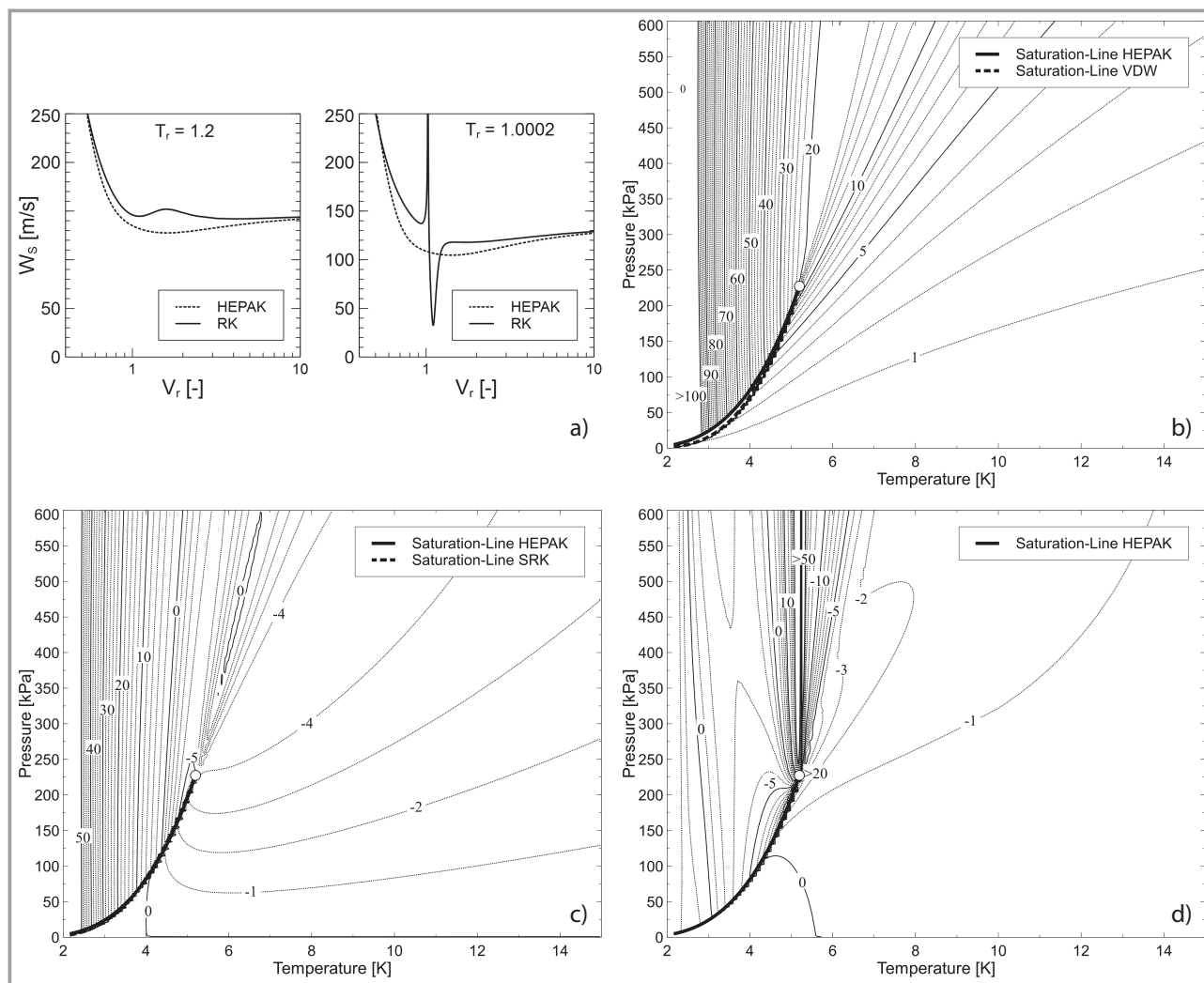


Figure 11. a) Speed of sound as a function of the reduced volume near the critical point calculated using the Redlich-Kwong EoS and properties from HEPAK at a reduced temperature of $T_r = 1.2$ (left) and $T_r = 1.0002$ (right), respectively. Error margins in % resulting from the computation of the speed of sound of helium when using b) the van der Waals EoS, c) the Soave-Redlich-Kwong EoS, or d) the EoS given by McCarty to solve Eq. (20). The primary results were held against reference values generated with the software package HEPAK.

limited range within which the polynomial expression that makes the attractive term of cubic EoSs temperature-dependent produces useful results. The one for the PR EoS fails miserably for values of $\omega < 0.2$ while the one for the SRK EoS is functional throughout the range $-0.5 < \omega < 0.5$. However, considering that $Z_c = 0.333$ for the SRK EoS and $Z_c = 0.3074$ for the PR EoS (see Tab. 1 for either of them), while the reference value for helium is $Z_c = 0.305$, better results from the PR EoS than from the SRK EoS would have been expected. As was shown in the discussion of the liquid densities at phase equilibrium, there is a general tendency to overpredict these densities uniquely related to helium. In these terms, the SRK EoS simply works more closely to the VdW EoS.

One difficulty in the design of safety valves for cryogenic helium lies in the high costs of practical tests so that their successful operation can often be proven only theoretically

and based on CFD simulations previously validated with practical tests using pressurized air. As suggested by the data in Tabs. S2 and S3, the relation of the mass flow rates between ambient air and cryogenic helium lays consistently around 2.75. In our CFD simulations, however, we found ratios that were smaller than this value and closer to 2.0.

Correspondingly, the maximum lifting forces for valve opening appear to be about 35 % higher for cryogenic helium than for air. This is what our calculations show for identical rates of friction. If frictional effects are stronger in flow patterns of cryogenic helium than in those with air, as possibly indicated by the higher Reynolds numbers and, therefore, by a higher proclivity to exhibit trans-sonic flow and dissipation by shock wave patterns, then these lifting forces are brought down to be about equal to the ones with air. As Tab. S3 and Fig. 14 indicate, helium flow rates by a factor of two higher than air flow rates in identical ducts are obtained

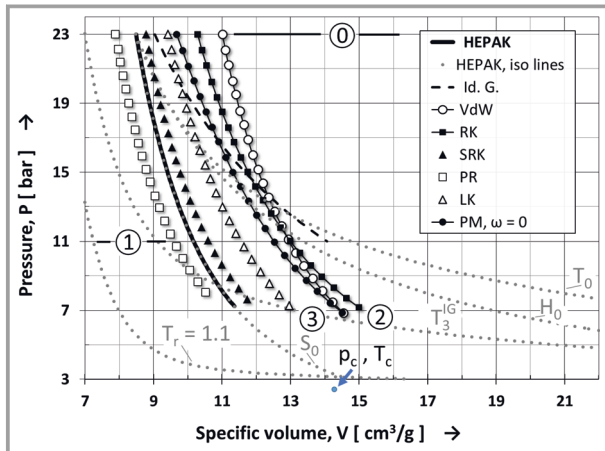


Figure 12. Volumetric data of helium as modeled for an adiabatic expansion beginning at $P_0 = 23$ bar and $T_0 = 10$ K, passing an intermediate pressure of 11 bar, and ending at sonic flow conditions. The expansion is not affected by frictional losses so that $r_f = 0$, which is why choked flow coincides with sonic flow. The results of various models can be compared to those obtained from the package HEPAK.

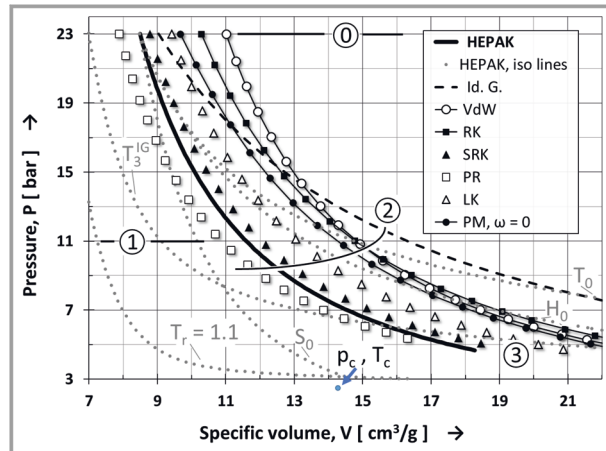


Figure 14. Volumetric data of helium as modeled for an adiabatic expansion beginning at $P_0 = 23$ bar and $T_0 = 10$ K, passing an intermediate pressure of 11 bar, and ending at sonic flow conditions. The expansion is affected by frictional losses of $r_f = 50\%$, why choked flow is reached before sonic flow. The results of various models are held against those obtained from the package HEPAK.

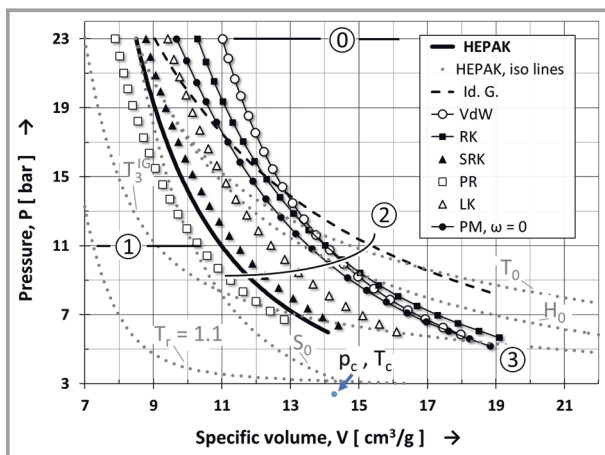


Figure 13. Volumetric data of helium as modeled for an adiabatic expansion beginning at $P_0 = 23$ bar and $T_0 = 10$ K, passing an intermediate pressure of 11 bar, and ending at sonic flow conditions. The expansion is affected by frictional losses of $r_f = 30\%$, why choked flow is reached before sonic flow. The results of various models are held against those obtained from the package HEPAK.

when the friction rate is increased to $r_f = 0.5$ for helium while the one for air is held at $r_f = 0.3$. Interestingly, in such a comparison, lifting forces are very well comparable between air flow and helium as are the overall dissipation rates $\dot{P}_{\text{diss},30,2} = \dot{m}_{30,2} W_{\text{diss},2}$ (here for a circular cross section with a diameter of 30 mm).

4 Conclusion

It could be shown and illustrated that a satisfactorily accurate representation of a fluid's density throughout its liquid and near-critical region can be best achieved by multi-parameter equations of state (MPEoSs) or fundamental EoSs, while cubic EoSs often produce unacceptable deviations from known reference values. Accordingly, the picture is quite similar and possibly even more pronounced when looking at variables from higher integrals or derivations of the density such as the heat of evaporation or the speed of sound. Fortunately, fundamental equations of state for numerous fluids, among which are water, carbon dioxide, and helium, have been developed and published, and are widely accepted as industry standard.

However, from understanding the underlying mathematical concepts of various equations of state it becomes obvious that higher MPEoSs or fundamental EoSs require much more mathematical effort to be resolved for the variables in question. While the quest for a thermodynamic variable of state is still relatively well manageable in any case as long as it has the format $X(V,T)$ or $X(P,T)$, CPU times increase by another factor of 3–5 when looking, e.g., for $Y(P,S)$ or $Z(H,S)$.

In today's world, where carrying out numerous practical experiments or testing functional parts over a wide variety of geometric parameters is often considered less desirable than performing appropriate simulations, beginners in this field are sometimes overwhelmed by the question: What is appropriate, what is feasible, and what could be achievable for me? Trying to do all the programming work on your own is as hopeless as the uninformed entry into a complex prefabricated software package can quickly become a blind flight – with a disastrous outcome as a rule. The contexts

presented here could guide a kind of self-empowerment that is rewarding under procedural as well as economical aspects.

In our experience, there are only three key points to observe: 1) Stay with the simplest EoS justifiable for your application until everything else runs fine. 2) When upgrading to an EoS of higher accuracy consider generating your own algorithms or look-up tables as well as plugging them in from external sources. 3) When evaluating or discussing the results of your rather complex simulations, awareness of the limitations of the EoS invoked by the former should prevent everyone from jumping to conclusions.

When we were concerned with the design of customized safety valves for near-critical cryogenic helium, we encountered significant difficulties in our CFD modeling work. We were able to solve them by using the SRK EoS in order to have the CFD algorithm converge on a flow pattern that we later used as initial conditions for a re-fined run. Here, we used the software package HEPAK [28] to generate look-up tables later accessed and invoked by the CFD code.

Supporting Information

Supporting Information for this article can be found under DOI: <https://doi.org/10.1002/cite.202100004>.

The authors are grateful for the support of their work by WEKA AG, Bäretswil, Switzerland.



After an apprenticeship as a machinist, Martin König studied Mechanical Engineering at the Zurich University of Applied Sciences (ZHAW) in Winterthur, Switzerland. He earned his B.Sc. degree in Mechanical Engineering in 2012. Then, he joined the Institute of Energy Systems and Fluid Engineering (IEFE) where he was working on thermo-

dynamic and fluid-mechanic aspects within research projects related to refrigeration plants, turbo machinery, etc. During this time, he also successfully earned his M.Sc. degree in Engineering within the MSE program. Martin König continued his work as a researcher at the IEFE for several years before improving his knowledge and mental involvement in martial arts as well his language skills in Japan for two years. He currently works as a process engineer for Schmid AG energy solutions (Eschlikon TG, Switzerland) in the field of wood combustion.



Markus Weber Sutter earned both his degree as eidg. dipl. Masch.-Ing. and his Dr. sc. techn. degree from the Swiss Federal Institute of Technology (ETH) in Zürich, Switzerland, in 1991 and in 1997, respectively. After his doctoral thesis with Prof. C. Trepp, he spent one year in Prof. Debenedetti's group at Princeton University (NJ) and another two years with Prof. Marc Thies at Clemson University (SC). After four years of working for Degussa Company in Hanau, Germany, and another two years for Levitronix company in Zürich, he accepted a position as a full-time lecturer at the Zürich University of Applied Sciences (ZHAW) in Winterthur in 2007, where he works on a variety of industry-related research projects mostly in the field of complex thermal applications.

Symbols used

a	$[\text{Pa m}^6 \text{mol}^{-2}]$	attraction term in cubic EoSs, e.g., van der Waals' EoS, Eq. (3)
a	$[\text{Pa m}^9 \text{mol}^{-3}]$	parameter in the EoS of Benedict, Webb, and Rubin, Eq. (6)
a	$[\text{J mol}^{-1} \text{K}^{-1}]$	coefficient for a polynomial of the heat capacity, Tab. 2
A	$[-]$	parameter in August's vapor pressure function, Eq. (23)
A_0	$[\text{Pa m}^6 \text{mol}^{-2}]$	parameter in the EoS of Benedict, Webb, and Rubin, Eq. (6)
a_1 – a_{20}	[various]	coefficients for the polynomials of the Bender EoS, Eq. (7)
b	$[\text{m}^6 \text{mol}^{-2}]$	parameter in the EoS of Benedict, Webb, and Rubin, Eq. (6)
b	$[\text{m}^3 \text{mol}^{-1}]$	inaccessible volume or repulsion term in cubic EoSs
b	$[\text{J mol}^{-1} \text{K}^{-2}]$	coefficient for a polynomial of the heat capacity, Tab. 2
B	$[\text{K}]$	parameter in August's vapor pressure function, Eq. (23)
B	$[\text{m}^3 \text{mol}^{-1}]$	coefficient in virial EoS, e.g., Eqs. (4) and (5)
B	$[\text{J m}^3 \text{mol}^{-2} \text{K}^{-1}]$	coefficient in EoS according to Bender, i.e., Eq. (7)
B	$[-]$	coefficient in EoS according to Lee and Kesler, i.e., Eq. (10)
B_0	$[\text{m}^3 \text{mol}^{-1}]$	parameter in the EoS of Benedict, Webb, and Rubin, Eq. (6)

c	$[\text{J m}^6\text{K}^2\text{mol}^{-3}]$	parameter in the EoS of Benedict, Webb, and Rubin, Eq. (6)	W	$[\text{J kg}^{-1}]$	process variable, specific work
c	$[\text{J mol}^{-1}\text{K}^{-3}]$	coefficient for a polynomial of the heat capacity, Tab. 2	Z	$[-]$	real-gas factor or compressibility coefficient
c	$[\text{m s}^{-1}]$	velocity	Greek letters		
C	$[\text{m}^6\text{mol}^{-2}]$	coefficient in virial EoS, e.g., Eqs. (4) and (5)	α	$[-]$	temperature correction of attractive term in cubic EoSs
C	$[\text{J m}^6\text{mol}^{-3}\text{K}^{-1}]$	coefficient in EoS according to Bender, i.e., Eq. (7)	α	$[\text{m}^9\text{mol}^{-3}]$	coefficient for the Benedict Webb Rubin EoS
C	$[-]$	coefficient in EoS according to Lee and Kesler, i.e., Eq. (10)	γ	$[\text{m}^6\text{mol}^{-2}]$	coefficient for the Benedict Webb Rubin EoS
C_p	$[\text{J mol}^{-1}\text{K}^{-1}]$	specific heat capacity at constant pressure	Γ	$[-]$	dimensionless specific Gibbs energy
C_v	$[\text{J mol}^{-1}\text{K}^{-1}]$	specific heat capacity at constant volume	δ	$[-]$	dimensionless density
C_0	$[\text{J m}^3\text{mol}^{-2}\text{K}^2]$	parameter in the EoS of Benedict, Webb, and Rubin, Eq. (6)	ε_p	$[-]$	deviation coefficient for the critical pressure in LK EoS
c_4	$[-]$	coefficient in EoS according to Lee and Kesler, i.e., Eq. (10)	ε_T	$[-]$	deviation coefficient for the critical temperature in LK EoS
d	$[\text{J mol}^{-1}\text{K}^{-4}]$	coefficient for a polynomial of the heat capacity, Tab. 2	η	$[-]$	dimensionless molar density for hard spheres in CS EoS
D	$[\text{m}^9\text{mol}^{-3}]$	coefficient in virial EoS, e.g., Eqs. (4) and (5)	κ	$[-]$	dimensionless polynomial expression for cubic EoSs
D	$[\text{J m}^9\text{mol}^{-4}\text{K}^{-1}]$	coefficient in EoS according to Bender, i.e., Eq. (7)	π	$[-]$	dimensionless pressure
D	$[-]$	coefficient in EoS according to Lee and Kesler, i.e., Eq. (10)	ρ	$[\text{mol m}^{-3}, \text{kg m}^{-3}]$	specific density
E	$[\text{J m}^{12}\text{mol}^{-5}\text{K}^{-1}]$	coefficient in EoS according to Bender, i.e., Eq. (7)	τ	$[-]$	dimensionless temperature
f	$[-]$	normalized vapor pressure function according to Lee and Kesler	Φ	$[-]$	dimensionless specific Helmholtz energy
F	$[\text{J m}^{15}\text{mol}^{-6}\text{K}^{-1}]$	coefficient in EoS according to Bender, i.e., Eq. (7)	χ	$[-]$	polar factor according to Halm and Stiel
F	$[\text{J mol}^{-1}]$	specific Helmholtz energy	ω	$[-]$	acentric factor according to Pitzer
G	$[\text{J m}^6\text{mol}^{-3}\text{K}^{-1}]$	coefficient in EoS according to Bender, i.e., Eq. (7)	Sub- and superscripts		
G	$[\text{J mol}^{-1}]$	specific Gibbs energy	(0)	referring to the simple fluid (which is argon), e.g., in Lee Kesler EoS	
$g_{j,i}$	[various]	coefficients for the generalized Bender EoS, Eq. (8)	attr	attractive	
H	$[\text{J m}^{12}\text{mol}^{-5}\text{K}^{-1}]$	coefficient in EoS according to Bender, i.e., Eq. (7)	c	critical, referring to the critical point	
H	$[\text{J mol}^{-1}]$	specific enthalpy	diss	referring to or due to dissipation	
M	$[\text{kg mol}^{-1}]$	molar mass, i.e., of an atom or a pure compound	f	friction	
P	[Pa]	(absolute) pressure	g, gas	gas, referring to the gaseous phase or state	
R	$[\text{J mol}^{-1}\text{K}^{-1}]$	universal gas constant, 8.3145	IG	ideal gas	
r_f	$[-]$	friction rate, $0 \leq r_f < 1$, Eqs. (29)–(32)	l, liq	liquid, referring to the liquid phase or state	
S	$[\text{J mol}^{-1}\text{K}^{-1}]$	specific entropy	P	referring to pressure or at constant pressure	
T	[K]	(absolute) temperature	r	reduced, meaning normalized by the appropriate critical value	
u	$[-]$	coefficient in generalized cubic EoS, i.e., Eq. (12)	(r)	of reference fluid (which is <i>n</i> -octane), e.g., in Lee Kesler EoS	
V	$[\text{m}^3\text{mol}^{-1}]$	specific volume	rep	repulsive	
w	$[-]$	coefficient in generalized cubic EoS, i.e., Eq. (12)	s	at saturation	
			snd	sound as in speed of sound	
			t	technical	
			T	referring to temperature or at constant temperature	
			vap	referring to or of vaporization	

Abbreviations

CS	EoS of Carnahan and Starling
EoS	equation of state
LK	EoS of Lee and Kesler
PM	EoS of Platzter and Maurer
PR	EoS of Peng and Robinson
RK	EoS of Redlich and Kwong
SRK	EoS of Soave, Redlich, and Kwong
VdW	EoS of van der Waals

References

- [1] J. D. van der Waals, *Over de Continuïteit van den Gas- en Vloeistoofstand*, Ph.D. Thesis, University of Leiden **1873**.
- [2] J. D. van der Waals, *The Equation of States for Gases and Liquids, in Nobel Lectures in Physics, Vol. 1: 1901–1921*, Elsevier, Amsterdam **1967**, 254–265.
- [3] B. E. Poling, J. M. Prausnitz, J. P. O'Connell, *The Properties of Gases and Liquids*, 5th ed., McGraw-Hill, New York **2000**.
- [4] R. Clausius, *Philos. Mag.* **1857**, *14*, 108–127. DOI: https://doi.org/10.1142/9781848161337_0009
- [5] J. C. Maxwell, *Philos. Trans. R. Soc. London* **1867**, *157*, 49–88. DOI: <https://doi.org/10.1098/rstl.1867.0004>
- [6] K. Lucas, *Angewandte Statistische Thermodynamik*, Springer, Berlin **1986**.
- [7] F. Schwabl, *Statistische Mechanik*, 3rd ed., Springer, Berlin **2006**.
- [8] K. Huang, *Statistical Mechanics*, John Wiley & Sons, New York **1987**.
- [9] E. Schrödinger, *Ann. Phys.* **1926**, *79* (6), 361–376. DOI: <https://doi.org/10.1002/andp.19263840602>
- [10] S. N. Bose, *Z. Phys.* **1924**, *26*, 178–181. DOI: <https://doi.org/10.1007/BF01327326>
- [11] T. Tél, *Z. Naturforsch., A: Phys. Sci.* **1988**, *43* (12), 1154–1174. DOI: <https://doi.org/10.1515/zna-1988-1221>
- [12] B. B. Mandelbrot, *Die fraktale Geometrie der Natur*, Springer, Basel **1987**.
- [13] K. S. Pitzer, *J. Am. Chem. Soc.* **1955**, *77* (13), 3427–3433. DOI: <https://doi.org/10.1021/ja01618a001>
- [14] N. F. Carnahan, K. E. Starling, *AIChE J.* **1972**, *18* (6), 1184–1189. DOI: <https://doi.org/10.1002/aic.690180615>
- [15] K. P. Johnston, C. A. Eckert, *AIChE J.* **1981**, *27* (5), 773–779. DOI: <https://doi.org/10.1002/aic.690270511>
- [16] S. Horstmann, A. Jabloniec, Krafczyk, K. Fischer, *Fluid Phase Equilib.* **2005**, *227* (2), 157–164. DOI: <https://doi.org/10.1016/j.fluid.2004.11.002>
- [17] H. Kamerlingh Onnes, in *KNAW, Proceedings, 4, 1901–1902*, Royal Netherlands Academy of Arts and Sciences, Amsterdam **1902**, 125–147.
- [18] M. Benedict, G. B. Webb, C. L. Rubin, *J. Chem. Phys.* **1940**, *8*, 334. DOI: <https://doi.org/10.1063/1.1750658>
- [19] R. Span, *Multiparameter Equations of State*, Springer, Berlin **2000**.
- [20] B. Platzter, G. Maurer, *Fluid Phase Equilib.* **1989**, *51*, 223–236. DOI: [https://doi.org/10.1016/0378-3812\(89\)80366-8](https://doi.org/10.1016/0378-3812(89)80366-8)
- [21] J. P. O'Connell, J. M. Haile, *Thermodynamics – Fundamentals for Applications*, Cambridge University Press, Cambridge **2005**.
- [22] W. Wagner, A. Kruse, *Properties of Water and Steam – The Industrial Standard IAPWS-IF97 for the Thermodynamic Properties*, Springer, Berlin **1998**.
- [23] R. Span, W. Wagner, *J. Phys. Chem. Ref. Data* **1996**, *25* (6), 1509–1596. DOI: <https://doi.org/10.1063/1.555991>
- [24] O. Kunz, W. Wagner, *J. Chem. Eng. Data* **2012**, *57* (11), 3032–3091. DOI: <https://doi.org/10.1021/je300655b>
- [25] S. Herrig, *New Helmholtz-Energy Equations of State for Pure Fluids and CCS-Relevant Mixtures*, Dissertation, Ruhr-Universität Bochum **2018**.
- [26] T. Holderbaum, J. Gmehling, *Fluid Phase Equilib.* **1991**, *70* (2–3), 251–265. DOI: [https://doi.org/10.1016/0378-3812\(91\)85038-V](https://doi.org/10.1016/0378-3812(91)85038-V)
- [27] R. L. Halm, L. I. Stiel, *AIChE J.* **1967**, *13* (2), 351–155. DOI: <https://doi.org/10.1002/aic.690130228>
- [28] *HEPAK*, version 3.40, Horizon Technologies, Littleton, CO **2005**.
- [29] R. D. McCarty, *J. Phys. Chem. Ref. Data* **1973**, *2* (4), 923–141. DOI: <https://doi.org/10.1063/1.3253133>
- [30] S. I. Sandler, *Chemical, Biochemical and Engineering Thermodynamics*, 4th ed., John Wiley & Sons, Hoboken, NJ **2006**.
- [31] O. Redlich, J. N. S. Kwong, *Chem. Rev.* **1949**, *44* (1), 233–244. DOI: <https://doi.org/10.1021/cr60137a013>
- [32] *Revised Release on the IAPWS Industrial Formulation 1997 for the Thermodynamic Properties of Water and Steam*, International Association for the Properties of Water and Steam **2007**.
- [33] *Advisory Note No. 1: Uncertainties in Enthalpy for the IAPWS Formulation 1995 for the Thermodynamic Properties of Ordinary Water Substance for General and Scientific Use (IAPWS-95) and the IAPWS Industrial Formulation 1997 for the Thermodynamic Properties of Water and Steam (IAPWS-IF97)*, International Association for the Properties of Water and Steam **2003**.

DOI: 10.1002/cite.202100004

Applying Common Equations of State to Three Reference Fluids: Water, Carbon Dioxide, and Helium

*Martin König, Markus Weber Sutter**

Review: Selecting an equation of state with a suitable trade-off between accuracy and manageability can be a crucial prerequisite when tackling the design of, e.g., safety valves for cooling applications operated with supercritical helium. One century of improvements of such equations is illustrated by a selection of significant comparisons. ■



Supporting Information
available online

